

Comparative research of electrospark deposited Tungsten alloy coating in two kinds of gas

Z. Liang^a, H. Zhang^a, S. Wang^{a,b,*}, L. Zhang^c, C. Zhu^d, H. Jin^{a,d}, C. Guo^a

^a*School of Equipment Engineering, Shenyang Ligong University, Shenyang 110159, China*

^b*State Key Laboratory of Explosion Science and Technology, Beijing Institute of Technology, Beijing 100081, China*

^c*Shandong Special Industry Group Co. Ltd, Zibo 255201, China*

^d*Chongqing Chang'an Industry (Group) Co. Ltd, Chongqing 401120, China*

A W alloy was used as an electrode to prepare a coating on a CrNi3MoVA steel substrate by means of electrospark deposition (ESD) technique. The mass transfer coefficient (MTC) from the electrode to the substrate was calculated through measuring the mass change by employing an electronic balance in air and in argon, respectively, and the morphologies, composition and phase structure were analyzed by utilizing scanning electron microscopy (SEM), energy dispersive X-ray spectrum (EDS) and X-ray diffraction (XRD). The results showed that the ambient gas has an obvious influence on the surface morphology, microstructure, phase structure and MTC of the ESD W alloy coating. Although the MTC in argon has a high value in the ESD process, the whole W alloy coating can't keep thickening as the ball-like bulges grow up on the surface, which will make the coating rough with the deposition time goes on.

(Received March 29, 2021; Accepted July 6, 2021)

Keywords: W alloy coating, Electrospark deposition, Mass transfer coefficient, Microstructure

1. Introduction

The wear of the key component of an equipment always happens on the surface and causes the equipment not work properly, so the performance improvement of the friction and wear of the component surface is a desirable problem to solve. Surface treatment techniques have been developed to enhance the properties of a component surface, and therefore prolong the serve life of the equipment [1-3]. The electrospark deposition (ESD) is a surface treatment technique to prepare strongly bonded coatings with excellent performance on metallic substrate materials. Except for metallurgically bonded coating, it has many advantages, such as low heat input in substrate, reproducible process, low cost, ambient friendly, etc [4-5]. This technology has been widely applied in the field of machinery, chemical industry, aviation, nuclear and military.

The ESD is a pulsed micro-arc welding process. In the ESD process, the electrode (anode) comes to contact the substrate (cathode) to momentarily produce a small melting pool on the substrate, and then the physicochemical reactions take place in the pool. As the ESD device generates heat in the 1% of a circle and radiates it via the surrounding in the remaining 99% of a circle due to short duration and high frequency, so the cooling rate can reach in the range of 10^5 - 10^6 °C/s. In such a rapid speed, the amorphous or nanocrystalline microstructure can be formed in the ESD coating. In recent reports, the ESD coatings with outstanding wear resistance include AlCoCrFeNi high-entropy alloy coating [6], Ni-MoS₂ self-lubricating coating [7], Zr-based amorphous-nanocrystalline coatings [8], etc. W alloy possesses high ultimate tensile strength, high hardness and high fracture toughness, so it is usually used as W alloy military swaging rod for armor piercing in military field [9]. However, to the best knowledge of the authors, there are still few research reports about the preparation of ESD W alloy coating.

* Corresponding author: zbgc2021@aliyun.com

Although the ESD technology has many advantages, its process parameters should be optimized for practical application. The two key factors, mass transfer coefficient (MTC) between anode and cathode, and gas ambient gas, must make clear before optimizing the process parameters, so the MTC of the ESD W alloy coating will be comparatively investigated in two kinds of gas.

2. Materials and methods

The CrNi3MoVA steel is selected as substrate material and its chemical composition shows in table 1. The bar of CrNi3MoVA steel was machined into cuboid-shape samples with a size of 10 mm×10 mm×3 mm, and the W alloy (W-5.25Ni-1.75Fe-0.3Co wt.%), sintered by powder metallurgy technology, was machined into cylinder-shape electrode with a size of Φ4 mm×20 mm by employing wire electrical discharge machining. The W coating was prepared by utilizing vibrating type ESD device, and its process parameters show in Table 2. The samples and electrode were ground to 800 grit finish by using SiC abrasive paper, and they were ultrasonically cleaned in ethanol and acetone mixture, and then immediately blew dry by a hair dryer before weighting. The original substrate and electrode were firstly measured by an electronic balance (Sartorius BP211D) with a sensitivity of 10^{-5} g, and then their mass changes were measured every minute.

Table 1. Chemical composition of CrNi3MoVA steel.

C	Mn	Si	Cr	Ni	Mo	V	S	P
0.40	0.41	0.25	1.28	3.14	0.37	0.20	0.001	0.012

Table 2. Processing parameters of ESD.

Power/W	Gas flow/L·min ⁻¹	Capacitance/μF
50	15	100

The equation of MTC:

$$K_t = \frac{\Delta_{kt}}{\Delta_{at}} \times 100\% ,$$

where K_t is the MTC, Δ_{kt} is the increased mass of the substrate, and Δ_{at} is the reduced mass of the electrode at time t .

The morphologies were obtained by scanning electron microscopy (SEM, Inspect F50, FEI Co., Hillsboro, Oregon), while the energy-dispersive spectrometer (EDS, X-Max, Oxford instruments Co., Oxford, UK) was utilized to analyse the chemical composition of the selected-area. The phase constitution of the coating was characterized by X-ray diffraction (XRD, X' Pert PRO, PANalytical Co., Almelo, Holland).

3. Results

3.1. MTC of W alloy coating in two kinds of gas

Fig. 1 shows the MTC of the W alloy coatings in two kinds of gas. As shown in Fig. 1, the MTC attains maximum value in two minutes in air, and then reduces gradually and attains negative value. The MTC firstly increases and then reduces in argon. After 4 min it attains maximum value, and then increases after reducing slowly. The MTC in argon keeps a high value during the whole deposition time. The maximum value in argon is 83.3% while that in air only 50.0%, which indicates that argon favors the material transfer from the electrode to the substrate.

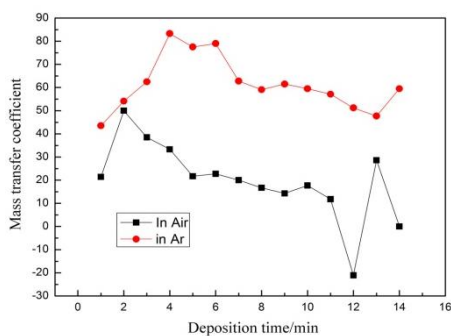


Fig. 1. MTC of the ESD W alloy coatings in two kinds of gas.

3.2. Surface morphologies of W alloy coating in two kinds of gas

Fig. 2 shows the surface morphologies of the ESD W alloy coating in air. As shown in Fig. 2a, the surface morphology is like orange peel and distributed with a lot of micro-holes (marked by arrows). The magnification of zone B (Fig. 2b) shows that there are a lot of micro-cracks on the surface of the coating. The EDS results of zone C have an average composition of (84.71W, 1.92Ni, 13.7Fe wt.%), indicating that a new alloy coating different from the electrode has been formed. The EDS results of point A in the micro-hole give strong O peaks, which suggests that oxidation took place in local zone when preparing W alloy coating in air.

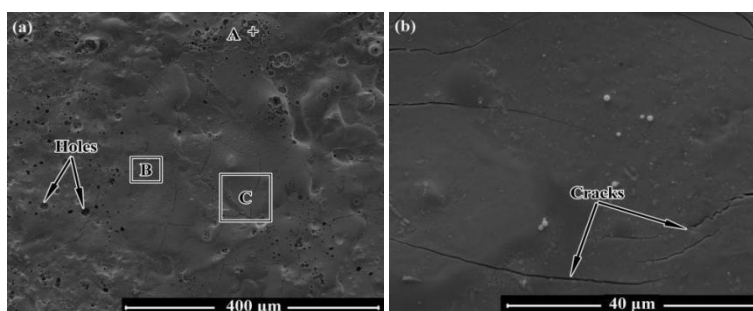


Fig. 2. Surface morphologies of low magnification (a) and magnification of zone B (b) of the ESD W alloy coating in air

Fig. 3 shows the surface morphologies of the ESD W alloy coating in argon. As shown in Fig. 3a, different from the morphology in air (Fig. 2a), a few ball-like bulges (marked by arrows) with a size of several hundred microns are distributed on the surface of the W alloy coating in argon. As shown in Fig. 3b, the EDS results (zone F) of the magnified ball-like bulge (zone D) have a composition of (93.81W, 4.48Ni, 1.71Fe wt.%) and approximates to the composition of the electrode, suggesting that the ball-like bulge was formed only by the self-deposition of the electrode. As shown in Fig. 3c magnified from zone E, different from the orange peel morphology in air (Fig. 2a), the metal spraying feature appears on the coating surface in argon. As shown in Fig. 3d magnified from zone Z, there is no micro-crack and only a feature of splashing metal solidification (marked by arrows) on the surface. The EDS results of zone G suggest that the W content of the coating in argon is almost the same as that of the coating in air.

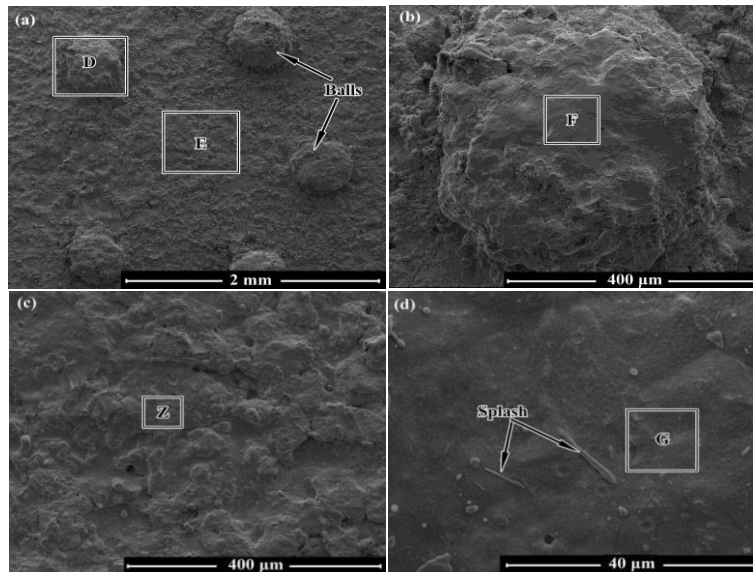


Fig. 3. Surface morphologies of low magnification (a) and magnification of zone D (b), zone E (c) and zone Z (d) of the ESD W alloy coating in argon.

3.2. Cross sectional morphologies of W alloy coating in two kinds of gas

Fig. 4 shows the cross sectional morphology and EDS results of the ESD W alloy coating in air. As shown in Fig. 4a, the thickness of the coating is about 20 μm , and the coating insets into the substrate and has a big fluctuant interface. There are a lot of variable-sized light pieces in the coating and inset black pieces on the surface of the coating. The element line profiles of W (Fig. 4b), Ni (Fig. 4c) and Fe (Fig. 4d) of the W alloy coating show that the element W and Fe are of gradient transition through the interface, indicating the metallurgically bonded coating was formed by the element mixing of the coating and the substrate. The EDS results of point H from the light piece are almost the element W, suggesting that local W aggregation appears in ESD process in air. The EDS results of point I from the gray zone show that the content of W in the coating is less than that on the coating surface and the content of Fe is the opposite, which is mainly due to the local W aggregation to reduce the W content of the gray zone. The EDS results of inset black piece on the surface of the coating give strong O peaks, combining with Fig. 2a and its EDS results, and suggests that the micro-holes were formed by the oxidation.

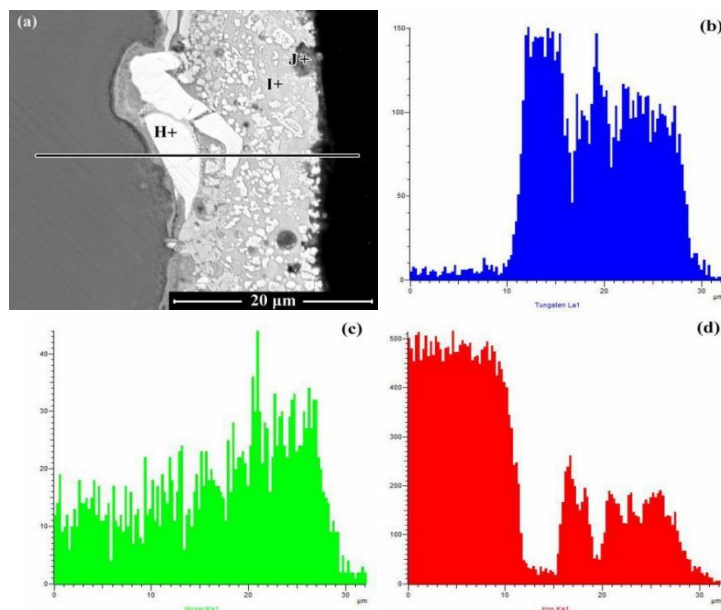


Fig. 4. Cross sectional morphology (a) and element line profiles of W (b), Ni (c) and Fe (d) of the ESD W alloy coating in air.

Fig. 5 shows the cross sectional morphologies of the ESD W alloy coating in argon. As shown in Fig. 5a, the thickness of the ball-like bulge is more than 200 μm , and there are big obvious cracks on its edge (marked by arrows). The magnified zone K (Fig. 5b) shows that the ball-like bulge with compact microstructure has columnar crystalline structure perpendicular to the substrate, and the nanocrystalline microstructure with a size of several tens of nanometers distributes within a columnar crystalline (marked by arrows). The EDS results of zone L have almost the same composition as the electrode, indicating that the electrode self-deposition formed the ball-like bulge. As shown in Fig. 5c without a ball-like bulge, in contrast to the cross sectional morphology of the coating in air (Fig. 4a), the coating in argon has an uniform microstructure and its interface is not fluctuant. The EDS results of zone M and N show that the element Fe reduces from middle to top in the coating and the change of the element W is the opposite.

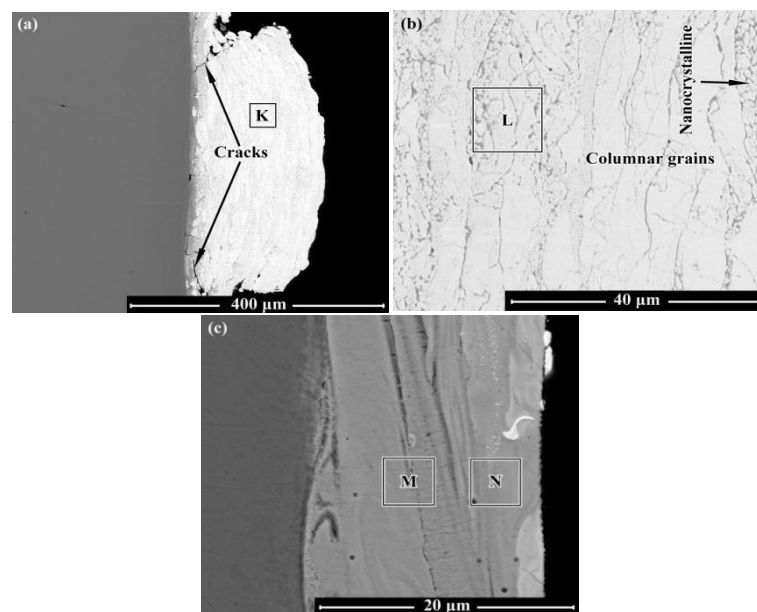


Fig. 5. Cross sectional morphologies of the ESD W alloy coating with a ball-like bulge (a), magnification of zone K (b) and without a ball-like bulge (c) in argon.

Fig. 6 shows the XRD patterns of the W alloy coating in two kinds of gas. As shown in Fig. 6, the W alloy coatings are both composed of α -W, α -Fe and γ -Fe(W) in two kinds of gas, but the peak of γ -Fe(W) in air has a left offset, compared with that of γ -Fe(W) in argon. According to Bragg diffraction formula, the W atoms dissolve into γ -Fe to cause the increase of atom radius in γ -Fe, i.e., the peak of γ -Fe will move towards left in the XRD patterns. The bigger angle value the peak moves, the more W atoms the γ -Fe dissolves. Therefore, in the ESD W alloy coating process, the γ -Fe dissolved more W atoms in air than the γ -Fe did in argon.

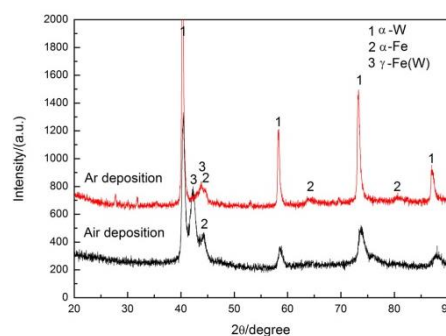


Fig. 6. XRD patterns of the W alloy coating in two kinds of gas.

Fig. 7 shows the surface morphologies of the electrodes after ESD. The surface morphology of the electrode after ESD in air (Fig. 7a) is flat and has many micro-holes, similar to that of the ESD W alloy coating in air (Fig. 2a). The surface morphology of the electrode after ESD in argon (Fig. 7b) is rough and has a splash feature, similar to that of the ESD W alloy coating in argon (Fig. 3c). The EDS results of zone O and P show that both electrode surfaces have a high content of element Fe, indicating the mass transfer from the substrate to the electrode happened.

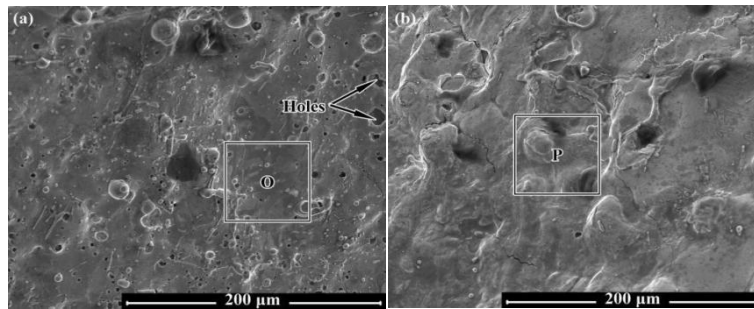


Fig. 7. Surface morphologies of the electrodes after ESD in air (a) and in argon (b).

4. Discussion

The ambient gas is ionized in the whole ESD process, so it has an obvious influence on the MTC value and coating microstructure. The ambient gas in this research includes air and argon. Air is a kind of dissociable gas and forms a plasma with high thermal conductivity in ESD process [10]. This plasma can make spheroidal melt produce at the tip of the electrode discharge, and then forms a small droplet to accelerate to the substrate, on the surface of which a small melting pool produces. Different from the electrode mass transfer mechanism in air, a plasma with low thermal conductivity forms in argon and can produce a spraying feature for the melt at the tip of the electrode. The spraying transfer produces more smooth and uniform deposition morphology than the spheroidal transfer does.

Fig. 8 shows the spark characterization of ESD in two kinds of gas. As shown in Fig. 8a, the spark color in air is yellow, and with the deposition time went on, the spark became weak gradually. As shown in Fig. 8b, the spark color in argon is glaring bright white, and forms a wide range of plasma between the electrode and the substrate, and this plasma with low thermal conductivity intensifies the mass transfer from the electrode to the substrate.

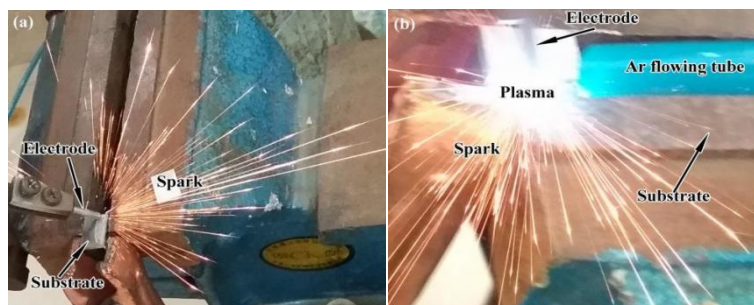


Fig. 8. Spark characterization of ESD in air (a) and in argon (b).

4.1. Gas influence on coating microstructure

Air is a kind of dissociable gas and its thermal conductivity is greater than argon's, so the cooling rate of ESD coating in air is higher than that in argon. On one hand, the higher cooling rate

can cause higher stress, and then the stress relieves by forming micro-cracks on the coating surface, as shown in Fig. 2b. On the other hand, the higher cooling rate makes the element W in the coating diffuse difficultly to produce W aggregation pieces, as shown in Fig. 4a. What's more, it causes W atom supersaturated solution in γ -Fe, and makes the peak of γ -Fe(W) move towards left more, as shown in Fig. 6. In contrast to ESD in air, ESD in argon makes the liquid metal in the melting pool have more time to solidify due to the spraying feature and low thermal conductivity plasma, which is beneficial for forming a coating with uniform microstructure.

X. Wei et al [11] found serious oxidation happened in the rough coating when they prepared Mo_2FeB_2 base cermet coating by means of ESD technique. However, in this experiment, except for the micro-holes on the coating surface, serious oxidation didn't happen in the coating. The main reasons are the high melting point of W alloy and the low melting point of its oxides, so even if the micro-holes formed on the surface of the coating and the electrode in the last ESD process, they would be eliminated in the next deposition process.

4.2. Gas influence on MTC

R. Wang et al [12] found that a new alloy coating was formed by the physicochemical reactions of the electrode and the substrate when they investigated the mass transfer law in ESD process. When the material of the electrode transfers to the substrate, a part of electrode material consumes in the ambient gas, and at the same time, a part of substrate material transfers to the electrode. Different pairs of electrode and substrate materials have different MTC values, which mainly is connected with the metallurgical properties of paired materials. When Q235 steel was selected as substrate, the MTC value of the Ni base alloy electrode approximated 80% while that of the WC-Co was only less than 20% in five minutes.

Except for the metallurgical properties of materials, the ambient gas has an obvious influence on the MTC value of the ESD in this experiment. In ESD process, small melting pools solidify as deposition micro-zones, and then they connect with each other to form a layer. After that, the electrode continues discharge to overlap on the formed layer. With the deposition time goes on, the micro-zones keep connecting and the layers keep overlapping. When the electrode firstly comes to contact the substrate, the metallurgical property of its surface has been changed, and after it finishes moving the whole substrate surface and the metallurgical property of the substrate surface has also been changed.

γ -Fe(W) is in the supersaturated state due to the higher cooling rate of liquid metal for the higher thermal conductivity in the ESD coating in air, and for the same reason the W atoms diffuse difficultly to aggregate to form α -W pieces. The coating will generate high thermal stress due to the high cooling rate, and then the cracks will form as the stress relieves. These cracks will produce more solid debris in the next discharge, which reduces the MTC value.

The elements have a gradient transition through the interface between the electrode and the substrate in the ESD W alloy coatings (Fig.4, Fig.5c), and with the deposition time goes on, the composition of the coating surface approximates to that of the electrode. As the ESD W alloy coating in air is mainly composed of α -W and supersaturated γ -Fe(W), the W atoms are difficult to dissolve into the supersaturated γ -Fe(W), which causes the low MTC value, and even negative MTC value. However, as the plasma in argon has low thermal conductivity and produces a spraying feature of liquid metal in a small melting pool, which makes the liquid metal has more time and better condition to mix and solidify. Therefore the microstructure of the W alloy coating in argon is uniform. In addition, the γ -Fe(W) in the W alloy coating in argon is not in the supersaturated state, and it will act as a binder when the liquid metal of the electrode solidifies in the layers in the next overlapping. Therefore the MTC value of W alloy coating in argon is higher.

Although the MTC value is higher in argon, with the deposition time went on, continuing deposition couldn't make the whole coating become thicker. Furthermore, the ball-like bulges grew up on the coating surface, which makes the coating rough and affects the coating performance. Hence the coating preparation should stop before the ball-like bulge grows up by means of ESD technique in argon.

5. Conclusions

1) There are many micro-cracks and micro-holes on the flat surface of the ESD W alloy coating, and a lot of α -W aggregation pieces in the ESD W alloy coating in air; a spraying feature appears on the surface of the ESD W alloy coating, and the microstructure is uniform in the ESD W alloy coating in argon.

2) The ESD W alloy coating are both composed of α -W, α -Fe and γ -Fe(W) in two kinds of gas, and the γ -Fe(W) dissolves more W atoms in air than it does in argon.

3) The maximum MTC value of the ESD W alloy coating in air was only 50.0% while that in argon attained 83.3%, and the former became negative value whilst the latter kept a high value with the deposition time went on.

4) The whole W alloy coating couldn't keep thickening in argon, and only the ball-like bulges grew up on the surface of the coating and made the coating surface rough with the deposition time went on.

Acknowledgments

The authors are grateful for the financial support of the National Science Foundation of Liaoning Province of China (No.20180550353, 2019-ZD-0264), and the Supporting Project of Middle-young Aged Innovative Talents of Science and Technology of Shenyang City (RC190292), and the Supporting Project of Innovative Talents of Colleges and Universities of Liaoning Province (LR2019059), and the Research Innovation Team Building Program of Shenyang Ligong University.

References

- [1] M. Shen, S. Zhu, F. Wang, Nature Communication **13797**, 1 (2016).
- [2] Y. Liao, B. Zhang, M. Chen, M. Feng, J. Wang, S. Zhu, F. Wang, Corrosion Science **167**, 108526 (2020).
- [3] C. Guo, F. Zhou, M. Chen, J. Wang, S. Zhu, F. Wang, Journal of Materials Science & Technology **70**, 1 (2021).
- [4] Y. Xie, M. Wang, Journal of Alloys and Compounds **480** 454 (2009).
- [5] A. E. Kudryashov, D. N. Lebedev, A. Y. Potanin, E. A. Levashov, Surface & Coatings Technology **335**, 104 (2018).
- [6] C. Guo, Z. Zhao, F. Lu, B. Zhao, S. Zhao, J. Zhang, Digest Journal of Nanomaterials and Biostructures **13**(4), 931 (2018).
- [7] C. Guo, F. Kong, S. Zhao, X. Yan, J. Yang, J. Zhang, Chalcogenide Letters **16**(7), 309 (2019).
- [8] X. Hong, Y. Tan, C. Zhou, X. Ting, Z. Zhang, Applied Surface Science **356**, 1244 (2015).
- [9] R. Luo, D. Huang, M. Yang, E. Tang, M. Wang, L. He, Materials Science & Engineering A **675**, 262 (2016).
- [10] R. N. Johnson, G. L. Sheldon, Journal of Vacuum Science & Technology A **4**(6), 2740 (1986).
- [11] X. Wei, Z. Chen, J. Zhong, Q. Huang, Y. Zhang, Y. Zhang, Rare Metal Materials and Engineering **27**(4), 1199 (2018).
- [12] R. Wang, Z. Chang, Y. Qian, T. Zhang, X. Huang, Welding & Joining **11**, 21 (2004).